Protein Engineering vol.10 no.1 pp.31–37, 1997

Engineering protein mechanics: inhibition of concerted motions of the cellular retinol binding protein by site-directed mutagenesis

D.M.F.van Aalten[1], P.C.Jones[2], M.de Sousa[3] and J.B.C.Findlay

Department of Biochemistry and Molecular Biology, University of Leeds, Leeds LS2 9JT, UK and [3]Instituto di Ciencias Biomedicas Abel Salazar, Centro de Estudos de Paramiloidose, Porto, Portugal

[2]Present address: Department of Biomolecular Chemistry, University of Wisconsin, Medical School, 587 Medical Sciences Building, 1300 University Avenue, Madison, WI 53706-1532, USA

[1]To whom correspondence should be addressed

Recently we reported on the dynamic properties of the cellular retinol binding protein, a member of the fatty acid binding protein family. A few conserved glycines were identified as important for producing the conformational changes necessary for the uptake and release of retinol. Here, we describe a multidisciplinary analysis of a genetically engineered mutation of one of these glycines (Gly67), designed to inhibit an observed hinge bending motion. The correctly folded mutant protein is unable to bind retinol. Analysis of the molecular dynamics simulations of the mutant and wild type protein using the essential dynamics method shows that the mutation indeed inhibits the hinge bending motions which are important for retinol binding.
Key words: cellular retinol binding protein/essential dynamics/molecular dynamics/protein engineering/site-directed mutagenesis

Introduction

The recently introduced essential dynamics (ED) technique (Amadei *et al*., 1993), a method for analysing molecular dynamics (MD) trajectories, has been very useful in identifying biologically significant motions in proteins on the basis of computer simulations. Several important hinge bending motions were revealed in thermolysin (van Aalten *et al*., 1995), histidine containing protein (Scheek *et al*., 1995), the SH3 binding domain (van Aalten *et al*., 1996a), *ras*-p21 (L.V.Mello, D.M.F.van Aalten and J.B.C.Findlay, submitted), lipases (Peters *et al*., in press) and the cellular retinol binding protein (cRBP) (van Aalten *et al*., 1996b). For all these proteins, the large concerted motions revealed by ED could be linked directly to experimental results, thus validating this technique. Several common features in the motions of these different proteins emerged. In general, there are only very few large concerted motions in proteins. These motions consist of rigid body displacements of secondary structure elements, kept together by flexible links. Interestingly, glycines frequently occur in these joints and are highly conserved even in evolutionary distant members of the same protein family (van Aalten *et al*., 1995, 1996b; L.V.Mello, D.M.F.van Aalten and J.B.C.Findlay, submitted). The fact that they are often found in these hinge bending regions and are well conserved may have functional implications. Glycines are conformationally flexible residues, which can be found at any position in the Ramachandran plot (G.N.Ramachandran and V.Sasisekharan, 1968) and can thus easily undergo rotations around their ϕ and ψ torsion angles, effectively allowing hinge bending motions to occur. Here, we test this hypothesis by mutating a conserved glycine in cRBP.

cRBP (Figure 1), a member of the fatty acid binding protein (FABP) family, is an intracellular retinol transporter. It takes up retinol from the plasma retinol binding protein, possibly via a membrane embedded receptor (Sivaprasadarao and Findlay, 1994) and transports it to locations in the cell. holo-cRBP binds and releases retinol to an acyl transferase which esterifies retinol for storage in the liver (Herr and Ong, 1992). Biochemical studies have pointed towards a difference in the conformation between apo-cRBP and holo-cRBP (Herr and Ong, 1992; Jamison *et al*., 1994). This was further supported by ED calculations (van Aalten *et al*., 1996b) which also revealed the large concerted motions in cRBP as well as differences in these motions in apo-cRBP and holo-cRBP. The concerted motions in cRBP consisted of a hinge bending motion of strands D and E (see Figure 1) together with a motion of the second helix, opening and closing the retinol entry site. In holo-cRBP, this motion was linked to a correlated displacement of retinol towards this entry site. Analyses of hinge activity pointed to the conserved Gly67 (in the loop between the D and E loops) as the most active hinge residue in the protein. Here, we study the functional importance of this glycine by mutating it to a less flexible residue.

Materials and methods

Mutant design

As set out in the Introduction, it was our aim to design a mutant which would inhibit the main essential motions observed in cRBP (van Aalten *et al*., 1996b). We decided to mutate the glycine at position 67, which is conserved throughout the FABP family. This residue has been predicted to be one of the main hinge bending residues and is important for producing the conformational changes necessary for the uptake and release of the ligand, by allowing the D and E strands to move apart, creating a 'hole' in the structure (Figure 1). By mutating this Gly67 to another residue, the conformational freedom at this hinge position is expected to be reduced leading to a possible inhibition of the large concerted motions. The substituting residue at position 67 was chosen using the following criteria.

(i) It should be a hydrophilic residue, as the amino acid at position 67 is fully exposed to the solvent.

(ii) The ϕ,ψ torsion angles at position 67 should be inside or near allowed regions in the Ramachandran plot (G.N.Ramachandran and V.Sasisekharan, 1968) of the substituting residue.

(iii) The residue should have a high score against glycine in mutation scoring matrices like the Dayhoff (Dayhoff *et al*., 1978) and PAM-like (Gonnet *et al*., 1992) matrices.

Considering these criteria, serine seemed the most appropriate candidate. It is hydrophilic, the ϕ,ψ torsion angles at position

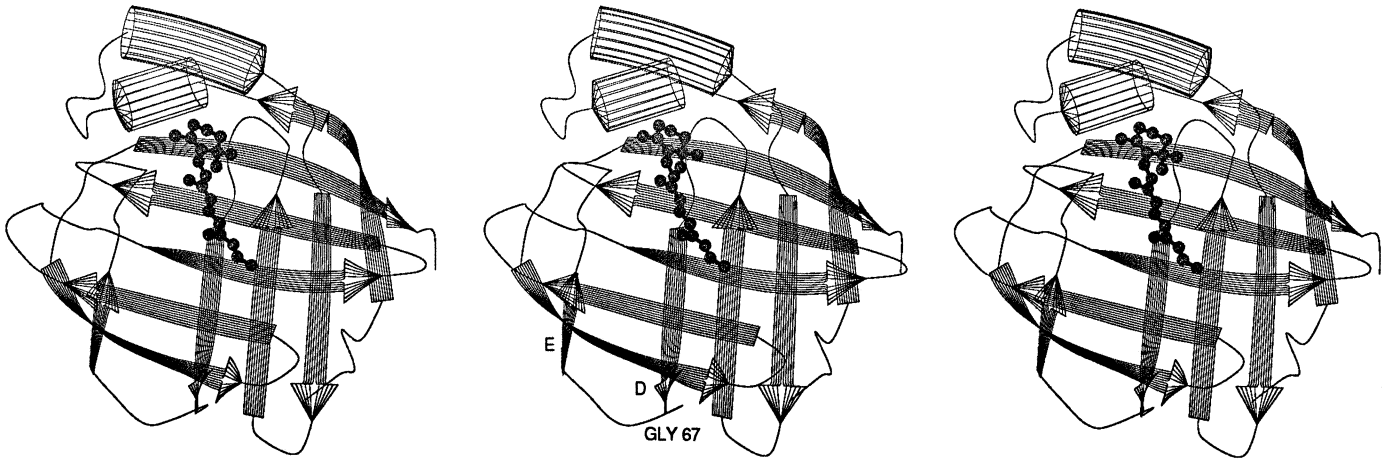

Fig. 1. Stereo picture of the cRBP topology, based on the crystal structure of holo-cRBP (Cowan *et al*., 1993). Gly67 and the hinge bending strands D and E are indicated. Retinol is drawn in a ball and stick representation.

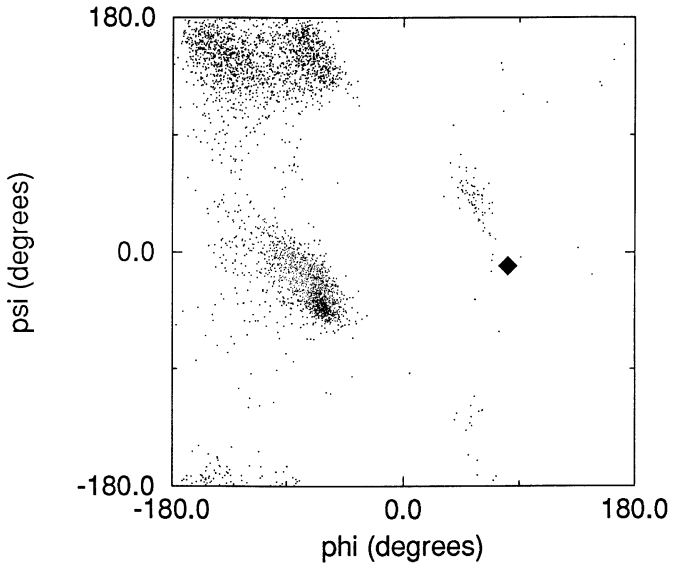

Fig. 2. Ramachandran plot of all serines occurring in the WHAT IF (Vriend, 1990) database of 285 high resolution X-ray structures (small dots) and Gly67 from the X-ray structure of cRBP (Cowan *et al*., 1993) (large diamond).

67 are close to an allowed region for serine (Figure 2) and it has the highest substitution scores with respect to glycine in the sequence homology matrices.

Insertion of human cRBP cDNA into a pT7.7 RNA polymerase/promoter plasmid

The total cRBP cDNA flanked by *Pst*I restriction sites was ligated using T4 DNA ligase (Boehringer Mannheim) in the *Pst*I site of the pKS I Bluescript plasmid (Stratagene). *Escherichia coli* XL1-Blue cells (Stratagene) were transformed with the ligation mixture and the clones were selected by their white colour on Luria–Bertani agar plates containing X-Gal, isopropylthio-β-galactoside (IPTG) and ampicillin. cRBP cDNA was then excised from the pKS-cRBP with *Eco*RI and *Bam*HI. Restriction of pKS-cRBP with *Bam*HI removes 128 bp of the 183 bp of the 3′ untranslated region. The resulting insert was ligated into the *Eco*RI and *Bam*HI sites of the pT7.7 RNA polymerase/promoter plasmid that contains the *E.coli* ribosomal binding site, to generate the pT7.7 cRBP construct.

A deletion polymerase chain reaction (PCR) (Sivaprasadarao and Findlay, 1993) was performed to remove the 5′ non-coding region of cRBP cDNA in pT7.7-cRBP and to fuse it to the translation initiation codon of the pT7.7 plasmid. The upstream primer represented bases +1 to +21 of the cRBP sequence (5′ CCA GTC GAC TTC ACT GGG TAC 3′) while the downstream primer was the reverse complement of the nucleotide −15 to +3 of the pT7.7 plasmid (5′ CTT CCT CTA TAT GTA TAC 3′). A mixture of 1 nmol of each of the two oligonucleotide primers was phosphorylated using 20 units of T4 polynucleotide kinase (Boehringer Mannheim) for 1 h at 37°C. The PCR was performed in a 100 µl volume using 50 pmol of each phosphorylated primer and 10 ng of pT7.7-cRBP, 0.2 mM dNTPs and 2.5 units *Pfu* DNA polymerase (Stratagene). Thirty PCR cycles, each consisting of 40 s at 94°C (denaturation), 1 min at 45°C (annealing) and 10 min at 72°C (extension), with a final extension for 10 min at 72°C were performed. The resulting product was purified from agarose gels with the gene clean kit II (Bioc 101) and self-ligated using T4 DNA ligase. Clones were sequenced to confirm deletion.

Construction of the Gly67 → Ser mutant

Site-directed mutagenesis was performed using a PCR-based approach (Landt *et al*., 1990). This method requires only one specific mutagenic primer (Gly67 → Ser) and a 5′ primer (FOR) and 3′ primer (REV) in the region of the plasmid flanking the coding region. The sequences of the primers used are as follows with the base change in the mutagenic primer underlined.

G67S 5′-CAAAC**<u>tcc</u>**TTGCTAACTTGGAAG-3′
FOR 5′-CGACTCACTATAGGGAGACC-3′
REV 5′-CCTCACTGATTAAGCATTGG-3′

The 5′ FOR primer and the Gly67 → Ser mutagenic primer were used in the first PCR reaction. The product was purified from an agarose gel by the method of Heery *et al*. (1990). In the second round of the PCR, the sense strand of this product served as a 5′ mutagenic mega-primer with the REV primer acting as the 3′ primer. The product of the second PCR reaction was digested with *Xba*I and subcloned into pT7.7. The orientation and sequence was subsequently confirmed.

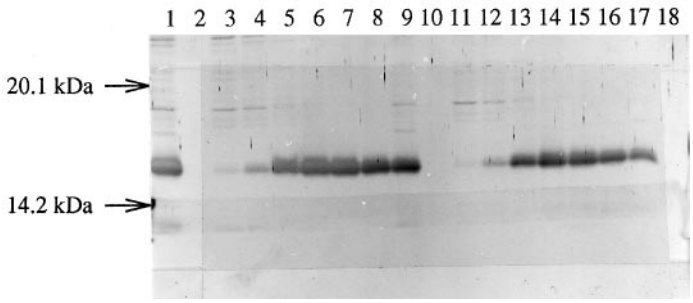

Fig. 3. Purification of the *E.coli*-derived WT and mutant cRBP. The WT and mutant cRBP were purified as described in Materials and methods. The Sephadex G-50 fractions were analysed by SDS–PAGE on a 15% gel and visualized by silver staining. Lanes 1–8 and lanes 9–18 represent the WT and mutant protein respectively. Lanes 1 and 9 show 1 µl of the treated and concentrated cell lysate (0.65 ml) for each protein. This concentrate was then applied to a Sephadex G-50 column and 1 ml fractions collected. Samples of 10 and 20 µl were analysed from the WT and mutant fractions respectively. Lanes 2 and 10 are from fraction 12 for each protein, lanes 3–8 and lanes 11–18 represent aliquots from fractions 14–19 for the WT protein and fractions 14–22 for the mutant respectively.

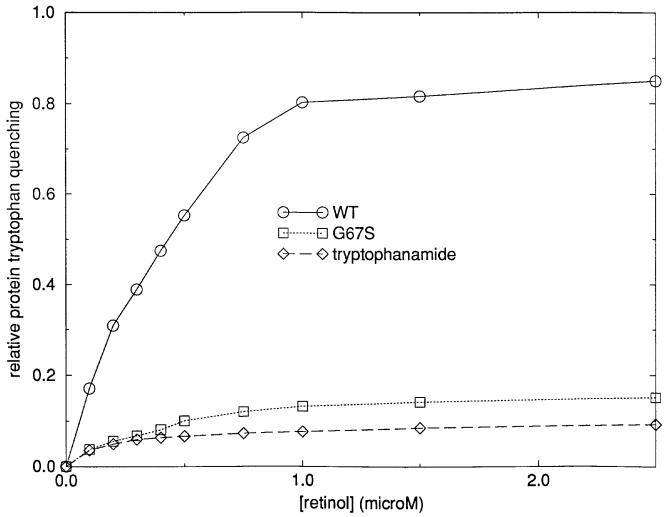

Fig. 4. Fluorescence quenching analysis of the WT, G67S and a standard tryptophanamide solution.

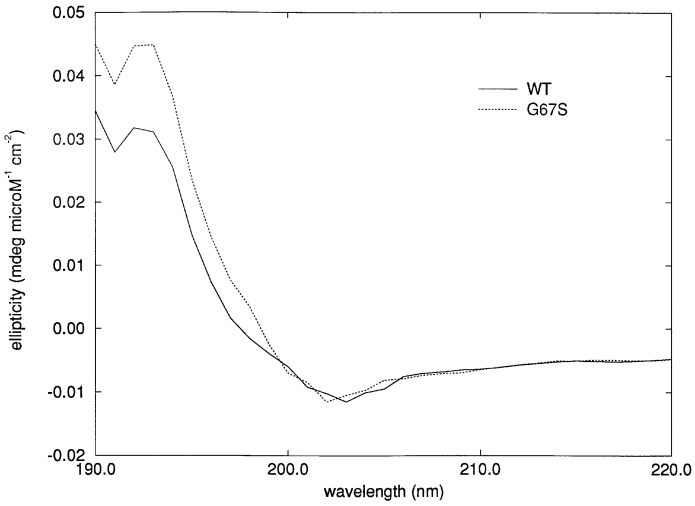

Fig. 5. CD spectra of the WT and G67S.

Expression and purification

Plasmids encoding wild type (WT) and the Gly67 → Ser mutant (G76S) were transformed into *E.coli* strain BL21(DE3) competent cells. The transformation was carried out as described by Inoue *et al*. (1990). Freshly transformed cells were grown overnight at 37°C and 200 r.p.m. in 5 ml 2YT broth containing 100 µg/ml of ampicillin (2YT/amp). Eighty microlitres were then used to seed 4 ml 2YT/amp and allowed to grow for 2 h at 37°C and 200 r.p.m. A further 16 ml 2YT/amp was then added and cells grown until an OD_{600} = 0.25 was reached. Expression was then induced by the addition of IPTG to a final concentration of 250 µg/ml. After growth for a further 3 h at 37°C and 200 r.p.m. the cells were harvested by centrifugation and the pellet frozen. The procedure used for purification follows a general outline first described for apo-cRBP II by Li *et al*. (1987). The cells were subsequently thawed and resuspended in 10 ml of cold buffer A (20 mM potassium phosphate, pH 7.4, 1 mM EDTA, 1 mM 2-mercaptoethanol, 0.05% sodium azide and 0.5 mM phenylmethanesulphonyl fluoride). A cell lysate was then prepared using a French press. The cell debris was pelleted by centrifugation at 30 000 *g* for 30 min at 4°C. SDS–PAGE, performed on a 15% acrylamide gel, using the buffer system of Schagger and von Jagow (1987), of a 20 µl aliquot of the supernatant showed cRBP to be the major band as revealed by Coomassie staining. Relatively large and small molecular weight proteins and impurities were removed by using a Centricon-100 and Centriprep-10 tubes (Amicon) respectively. The latter allows concentration and desalting to occur. cRBP was then purified from the concentrated sample by chromatography using a Sephadex G-50 column (1.5 × 30 cm) equilibrated with buffer A. Fractions were analysed by SDS–PAGE as described above and those estimated to be more than 95% pure from a silver-stained gel were used for further analyses.

All-trans retinol binding studies

Retinol binding was followed by monitoring the fluorescence emission of retinol and by the quenching of protein fluorescence. The procedures followed were as described previously (Li *et al*., 1987; Levin *et al*., 1988). Solutions of proteins were prepared at concentrations in the range 0.25–1.0 µM in buffer A. *N*-Acetyl-L-tryptophanamide (Sigma) was used as a blank. The binding affinity (K_d) was determined by fitting the data to a hyperbolic equation using non-linear regression by the program FIGP:

$$F = (F_{max}[S])/(K_d + [S]) \quad (1)$$

where F is the corrected fluorescence (the fluorescence of the protein minus the fluorescence of the corresponding *N*-acetyl-L-tryptophanamide sample), F_{max} is the calculated maximal fluorescence, K_d is the calculated Michaelis constant and [*S*] is the substrate concentration.

Circular dichroism

Purified protein in buffer A was freeze dried and resuspended in H_2O in a concentration range of 5–30 µM. The circular dichroism (CD) spectra were recorded using a path length of 0.1 mm. The procedures for analysis were similar to those described for cRBP (Zhang *et al*., 1992):

$$\theta_M = (\theta)/(C \times d) \quad (2)$$

where θ is the measured ellipticity in millidegrees, C is the molar protein concentration and d is the path length in cm.

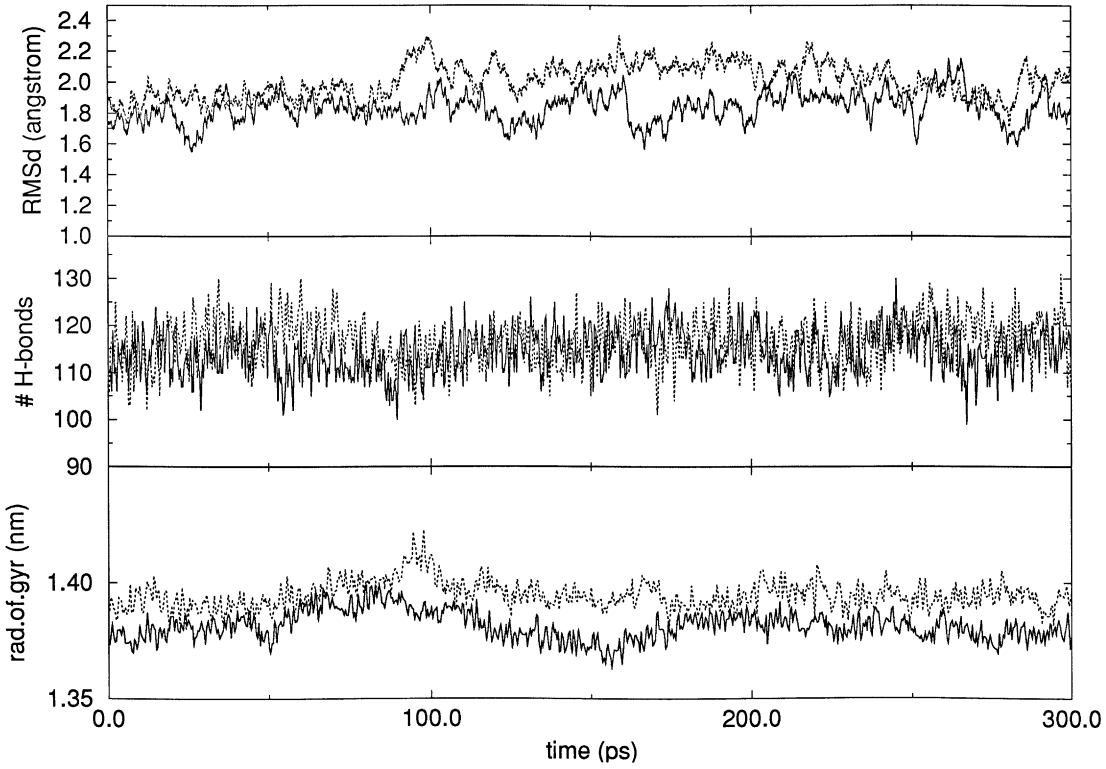

Fig. 6. Various properties monitored along the 300 ps equilibrium trajectories of the WT and G67S. Upper graph: the r.m.s.d. of the C_α positions with respect to the holo-cRBP crystal structure (Cowan *et al*., 1993). Middle graph: the total number of backbone hydrogen bonds. Lower graph: the radius of gyration.

Simulation details

All the energy minimization (EM) and MD runs were performed using the GROMOS program suite (van Gunsteren and Berendsen, 1987) as published previously (van Aalten *et al*., 1996b). In short, the simulation of the apo form of the wild type (WT) protein was started from the crystal structure of the holo form of cRBP (Cowan *et al*., 1993). The protein was simulated in a truncated octahedral periodic boundary box filled with 2547 SPC water molecules (Berendsen *et al*., 1981) (the total number of atoms was 10 087) at constant pressure (τ_p = 0.5 ps) and a temperature of 300 K (τ_T = 0.1 ps), for a time span of 300 ps (van Aalten *et al*., 1996b). SHAKE (Ryckaert *et al*., 1977) was applied to constrain bond lengths to their equilibrium values and a cut-off radius of 8 Å (10 Å for long-range electrostatic interactions) was used. Simulations were performed with modified carbon–water–oxygen interaction parameters (van Buuren *et al*., 1993).

G67S was constructed from the WT 100 ps simulation structure. The serine was modelled using the standard rotamer from the WHAT IF rotamer library (Vriend, 1990). The simulation was then continued using continuation parameters identical to those used in the WT simulation. After 100 ps of equilibration, a 300 ps trajectory was produced which was used for comparisons to the 300 ps WT trajectory.

The structures and trajectories were visualized with WHAT IF (Vriend, 1990). The geometrical properties were calculated from the WHAT IF trajectory analysis menu, using DSSP (Kabsch and Sander, 1983).

Essential dynamics

The ED method (Amadei *et al*., 1993) is able to extract the large concerted motions of atoms from an MD trajectory. The first step involves the construction of a covariance matrix

$$C_{ij} = < (x_i - x_{i,0})(x_j - x_{j,0}) > \quad (3)$$

where $x_{i,j}$ are the separate *x*, *y* and *z* coordinates of the atoms and x_0 the average values of the coordinates (calculated over the whole trajectory, after all the frames were fitted onto a reference structure to remove the overall translational and rotational motion). This covariance matrix is then diagonalized, yielding a set of eigenvalues and eigenvectors. The eigenvectors indicate directions in a $3N$ dimensional space (with N = number of atoms), that is the concerted fluctuations of the atoms. The eigenvalues are equivalent to the total mean square displacement of the atoms along their corresponding eigenvectors. In the case of proteins, there are always only a few eigenvectors with large eigenvalues, i.e. with only a few eigenvectors the large overall motion of the protein can be described adequately (Amadei *et al*., 1993; van Aalten *et al*., 1995, 1996a,b).

A useful method for comparing the ED of two simulations on similar systems is the so-called 'combined' analysis (van Aalten *et al*., 1995). In this method, two or more trajectories, fitted onto the same reference structure, are concatenated and a covariance matrix is constructed. The two separate trajectories are then projected onto the resulting eigenvectors and the properties of these projections are compared for the two simulations. Two properties can be studied.

(i) The average projection, which might reveal different average displacements along the eigenvectors, i.e. the simulations have a different equilibrium structure in that direction ('static shift').

(ii) The mean square fluctuation in the projection, showing possible differences in dynamics along the eigenvector direction ('dynamic shift'). Here, this method is applied to the concatenated trajectories of the WT and G67S.

Results

Construction and analysis of the G67S

The WT and G67S were expressed in *E.coli* and purified as described in the Materials and methods. The transcription was regulated by the T7 RNA polymerase promoter, with expression being induced upon the addition of IPTG. The levels of expression were maximal with the WT (20 mg/ml) and lower with G67S (4 mg/ml). An SDS–PAGE analysis of the protein derived from Sephadex G-50 gel filtration revealed fractions that contained only cRBP as judged by silver staining (Figure 3). The lack of absorbance at a wavelength >310 nm indicated that both proteins were free of retinol (data not shown).

Fluorimetric titrations were used to determine the effect of the mutation on the binding affinity for the all-*trans* retinol. Two methods were used. The quenching of intrinsic (tryptophan) fluorescence was monitored by exciting the protein at 290 nm and monitoring the fluorescence at 340 nm upon the addition of retinol. Secondly, the increase in the retinol fluorescence upon binding to the protein was followed by exciting at 350 nm and measuring the emission at 490 nm. The results from both analyses were similar showing that the WT bound retinol with a K_d = 160 nM but that G67S bound the ligand only very weakly, if at all. The decrease in protein fluorescence for G67S is slightly larger than that of the control solution containing *N*-acetyl-L-tryptophanamide and slightly greater when monitoring the retinol fluorescence. It was not possible to determine a K_d from such data. In addition, an absorbance scan did not reveal any absorbance attributable to the bound retinol. Figure 4 shows the effect of the increasing concentration of retinol on the WT and mutant protein and on the *N*-acetyl-L-tryptophanamide solution.

Such results could arise from the incorrect folding of the mutant protein. However, an identical elution profile on gel filtration would suggest that the Stoke's radius is largely unaffected and that no major perturbations exist. In order to verify that G67S had folded correctly, both the WT and mutant protein were analysed by CD. The CD spectra for both forms were almost identical (Figure 5). Such spectra have been shown to be indicative of a highly ordered β structure (Zhang *et al.*, 1992) for the highly homologous cRBP and suggest that the overall structures are comparable.

Stability of the simulations

The stability of the G67S simulation was assessed by calculating several geometrical properties. The root mean square deviation (r.m.s.d) of the C_α carbons with respect to the holo-cRBP crystal structure (Cowan *et al.*, 1993), the total number of hydrogen bonds and the radius of gyration all seem to be stable, fluctuating around a mean (Figure 6). These properties show that the simulation is stable and may be used for ED analyses.

Essential dynamics

The 300 ps equilibrium trajectories for the WT and G67S were concatenated and fitted onto a reference structure to remove the overall translational and rotational motions. A covariance matrix was constructed from the C_α coordinates taken from this fitted trajectory. As usual (Amadei *et al.*, 1993; van Aalten *et al.*, 1995, 1996b), upon diagonalization of the covariance matrix only a few eigenvectors with high eigenvalues were obtained, indicating a low-dimensional essential subspace. These eigenvectors indicate identical motions in the WT and G67S trajectories, since the covariance matrix was constructed from both trajectories together. The structural and dynamic effects of the mutation can now be studied by considering the projections of the separate WT and G67S trajectories on these 'combined' eigenvectors. The average projections (revealing the possible structural effects) and the mean square fluctuations in these projections (revealing the possible dynamic effects) are shown in Figure 7. These properties of the projections reveal two main effects.

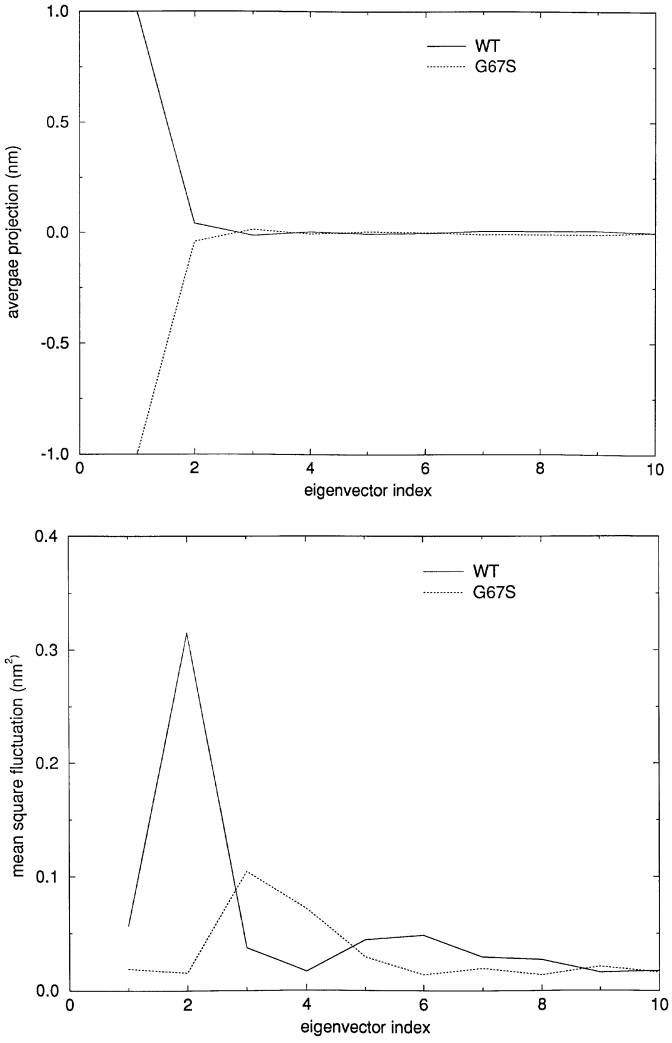

Fig. 7. (**A**) Average projection of the MD simulation time frames of the separate WT and G67S trajectories onto the eigenvectors calculated from the combined trajectory. (**B**) Mean square fluctuation in the projection of the MD simulation time frames of the separate WT and G67S trajectories onto the eigenvectors calculated from the combined trajectory.

(i) A structural effect: on average, the WT and G67S simulations are at different positions along eigenvector 1 (Figure 7A). Thus, there is some conformational change caused by the mutation. The simulation structures at the extremes of this eigenvector (i.e. those with the overall minimum and maximum projections) are shown in Figure 8. The D and E strands (and the C–D and E–F loops) seem to have moved towards each other, effectively partially closing the retinol entry site.
(ii) A dynamic effect: the dominating difference in fluctuation is along the direction described by eigenvector 2 (Figure 7B). Thus, there is a motion which is the largest (the most essential) motion in the WT simulation, but which is almost completely

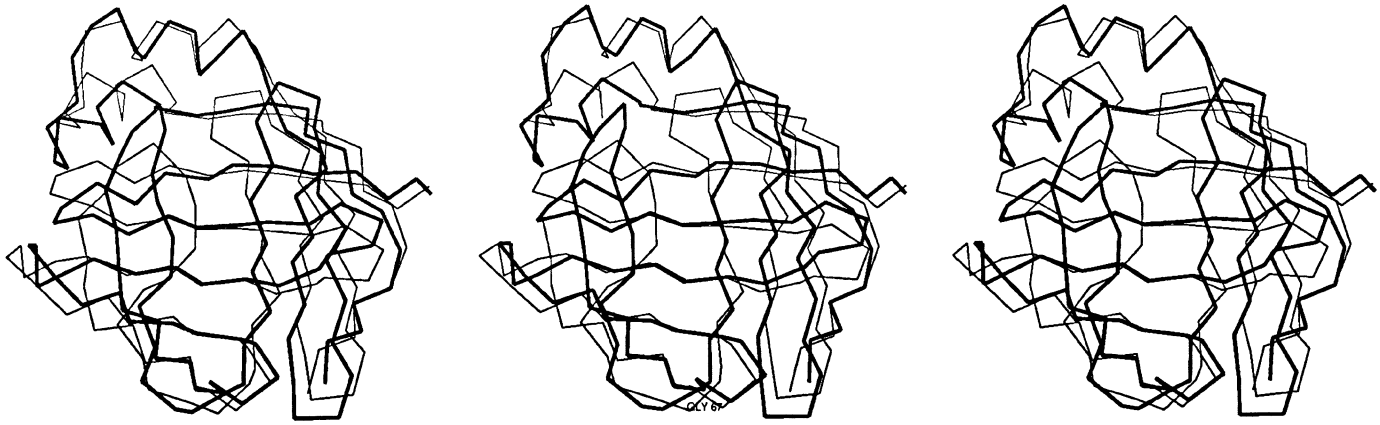

Fig. 8. Stereo picture of the superposition of the minimum (corresponding to G67S, thin line) and maximum (corresponding to WT, bold line) projection structures of eigenvector 1 (see also Figure 7A).

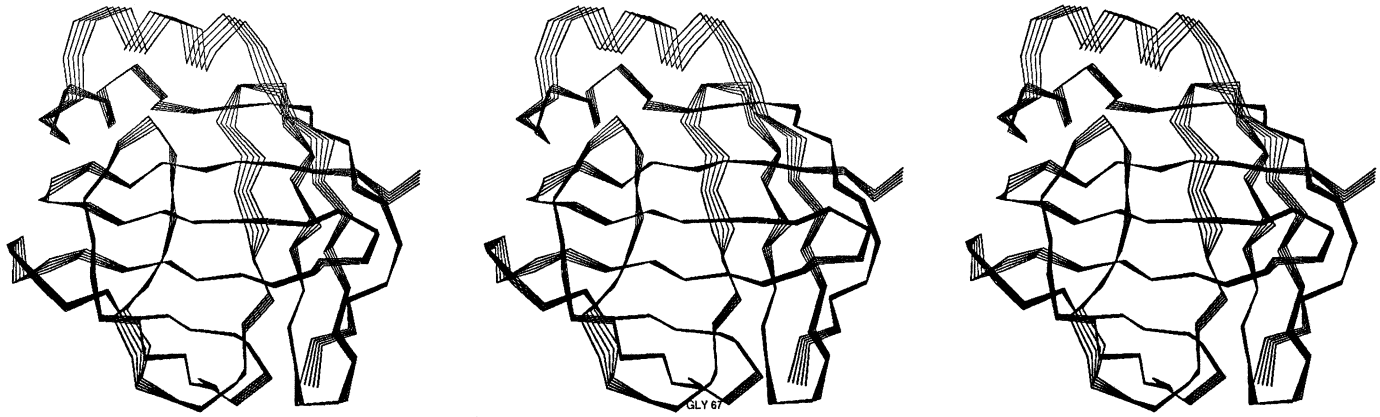

Fig. 9. Stereo picture of the superposition of five structures depicting the concerted motion described by eigenvector 2.

inhibited in the G67S simulation. The concerted motion described by this eigenvector is shown in Figure 9. It is similar to the essential motions in apo-cRBP and holo-cRBP described earlier (van Aalten *et al.*, 1996b): a concerted motion of the second helix together with the hinge bending motion of the D and E strands, which effectively control the opening to the ligand binding site.

Discussion and conclusions

The multidisciplinary approach taken here has provided further insight into the dynamic behaviour of cRBP. Previous ED analyses have hinted at an important role for the conserved glycine at position 67. The ED and biochemical analyses (which were done in parallel) of the Gly67 $\rightarrow$ Ser mutant presented here are consistent and confirm the importance of this glycine for the cRBP (and possibly other FABPs) function.

The mutant was designed such that a large structural effect was not to be expected. Indeed, the similar CD spectra (Figure 5) and the similar Stoke's radii indicate that the G67S is properly folded. A small structural effect (which would not change these properties) is observed in the ED analyses (Figure 7A), partially closing the entry site to the ligand pocket. The main effect observed by ED, however, is a change in the dynamic behaviour (Figure 7B). A motion which has been implied as important for retinol binding and release has been inhibited by the mutation. This is consistent with the binding data: cRBP has essentially lost its ability to bind retinol. It was shown previously that the large concerted motions in cRBP are inhibited in the holo form and enhanced in the apo form (van Aalten *et al.*, 1996b). The latter effect is functionally significant: a large fluctuation of these loops means occasional larger openings of the retinol entry site and this increases the chance of retinol entering its binding pocket. The mutation described here inhibits these fluctuations, thus significantly reducing the chance of retinol uptake.

Others have also investigated the importance of conserved glycines in flexible loops in dihydrofolate reductase (Gekko *et al.*, 1993, 1994), serpin (Hopkins *et al.*, 1993) and glutathione synthetase (Tanaka *et al.*, 1993). These studies also point towards the possible importance of conserved glycines for protein function. Their approaches differ, however, in several ways from ours. First, the mutations were selected rather randomly, without proper regard for the local conformation or accessibility. Indeed, this resulted in significant structural changes as is evident from the CD spectra (Gekko *et al.*, 1993, 1994; Tanaka *et al.*, 1993). Here, we have tried to avoid large structural effects by using a rational mutant design. Second, their glycines were in large mobile loops, whereas the D–E loop in cRBP is small and rather static, mainly allowing flexibility to occur only at Gly67. This is the first report on the use of the essential dynamics technique to study the possible effects of the mutated hinge bending residues on the dynamic behaviour of the protein. If it is possible to identify residues which are important for the functional motions of

protein reliably and also predict the effect of possible mutations, the ED technique can prove to be useful as a general mutant prediction tool.

Conserved glycines acting as hinge bending residues in the large concerted motions revealed by ED have been observed in other proteins (van Aalten *et al*., 1995; L.V.Mello, D.M.F.van Aalten and J.B.C.Findlay, submitted). We are currently conducting further mutagenesis and ED studies towards these glycines.

References

Amadei,A., Linssen,A.B.M. and Berendsen,H.J.C. (1993) *Proteins*, **17**, 412–425.

Berendsen,H.J.C., Postma,J.P.M., van Gunsteren,W.F. and Hermans,J. (1981) In Pullmann,B. (ed.), *Intermolecular Forces*. Reidel, Dordrecht, p. 331.

Cowan,C.W., Newcomer,M.E. and Jones,T.A. (1993) *J. Mol. Biol*., **230**, 442–446.

Dayhoff,M.O., Schwarz,R.M. and Orcutt,B.C. (1978) In Dayhoff,M.O. (ed.), *Atlas of Protein Sequence and Structure*. National Biomedical Research Foundation, Washington, DC, p. 345.

Gekko,K., Yamagami,K., Kunori,Y., Ichibara,S., Kodama,M. and Iwakura,M. (1993) *J. Biochem*., **113**, 74–80.

Gekko,K., Kunori,Y., Takeuchi,H., Ichibara,S. and Kodama,M. (1994) *J. Biochem*., **116**, 34–41.

Gonnet,G.H., Cohen,M.A. and Benner,S.A. (1992) *Science*, **256**, 1443–1445.

Heery,D.M., Gannon,F. and Powell,R. (1990) *Trends Genet*., **6**, 173.

Herr,F.M. and Ong,D.E. (1992) *Biochemistry*, **31**, 6748–6755.

Hopkins,P.C.R., Carell,R.W. and Stone,S.R. (1993) *Biochemistry*, **32**, 7650–7657.

Inoue,H., Nojima,H. and Okayama,H. (1990) *Gene*, **96**, 23–28.

Jamison,R.S., Newcomer,M.E. and Ong,D.E. (1994) *Biochemistry*, **33**, 2873–2879.

Kabsch,W. and Sander,C. (1983) *Biopolymers*, **22**, 2577–2637.

Landt,O., Grunert,H.P. and Hahn,U. (1990) *Gene*, **96**, 125–128.

Levin,M.S., Locke,B., Yang,N.C., Li,E. and Gordon,J.I. (1988) *J. Biol. Chem*., **263**, 17715–17723.

Li,E., Locke,B., Yang,N.C., Ong,D.E. and Gordon,J.I. (1987) *Gastroenterology*, **92**, 1506.

N,R.G. and V,S. (1968) *Adv. Protein Chem*., **23**, 283–437.

Peters,G.H., van Aalten,D.M.F., Edholm,O., Toxvaerd,S. and Bywater,R. (1996) *Biophys. J*., **71**, 2245–2255.

Ryckaert,J.P., Ciccotti,G. and Berendsen,H.J.C. (1977) *J. Comp. Phys*., **23**, 327–341.

Schagger,H. and von Jagow,G. (1987) *Anal. Biochem*., **166**, 368–379.

Scheek,R.M., van Nuland,N.A.J., de Groot,B.L. and Amadei,A. (1995) *J. Biomol. NMR*, **6**, 106–111.

Sivaprasadarao,A. and Findlay,J.B.C. (1993) *Biochem. J*., **296**, 209–215.

Sivaprasadarao,A. and Findlay,J.B.C. (1994) *Biochem. J*., **300**, 437–442.

Tanaka,T., Yamaguchi,H., Kato,H., Nishioka,T., Katsube,Y. and Oda,J. (1993) *Biochemistry*, **32**, 12389–12404.

van Aalten,D.M.F., Amadei,A., Vriend,G., Linssen,A.B.M., Venema,G., Berendsen,H.J.C. and Eijsink,V.G.H. (1995) *Proteins*, **22**, 45–54.

van Aalten,D.M.F., Amadei,A., Bywater,R., Findlay,J.B.C., Berendsen,H.J.C., Sander,C. and Stouten,P.F.W. (1996a) *Biophys. J*., **70**, 684–692.

van Aalten,D.M.F., Findlay,J.B.C., Amadei,A. and Berendsen,H.J.C. (1996b) *Protein Engng*, **8**, 1129–1135.

van Buuren,A.R., Marrink,S.J. and Berendsen,H.J.C. (1993) *J. Phys. Chem*., **97** (36), 9206–9212.

van Gunsteren,W.F. and Berendsen,H.J.C. (1987) *GROMOS Manual*. BIOMOS, Biomolecular Software, Laboratory of Physical Chemistry, University of Groningen, The Netherlands.

Vriend,G. (1990) *J. Mol. Graph*., **8**, 52–56.

Zhang,J.H., Liu,Z.P., Jones,T.A., Gierasch,L.M. and Sambrook,J.F. (1992) *Proteins*, **13**, 87–99.

Received May 13, 1996; revised July 29, 1996; accepted August 16, 1996